

## Single-centred calculations of excitation and electron removal in intermediate energy $p + H(n = 2)$ collisions

A L Ford, J F Reading and K A Hall

Center for Theoretical Physics, Physics Department, Texas A&M University, College Station, TX 77843, USA

Received 8 July 1993, in final form 28 September 1993

**Abstract.** Large-basis single-centred expansion calculations have been previously shown to yield accurate cross sections for collisions between protons and ground state hydrogen atoms. In the present paper the method is extended to  $p + H(n = 2)$  collisions. Cross sections for  $2s$  and  $2p \rightarrow 3l'$  and  $4l'$  excitation and for electron removal from  $2s$  and  $2p$  are presented and compared to other theoretical calculations.

### 1. Introduction

In the preceding paper (Ford *et al* 1993) we showed that coupled-states calculations carried out using a large target-centred basis yield accurate excitation and electron removal cross sections if a sufficient number of angular momenta are included in the basis. Application was made to  $p + H(1s)$  collisions, where there is experimental data and also extensive previous theoretical work. We obtained convergence of the cross sections with respect to the basis and the results were in generally good agreement with experiment and with other calculations for collision energies of 15 keV and above.

The present paper reports the results of similar calculations for excitation to  $3l'$  and  $4l'$  levels and for electron removal in collisions of protons with hydrogen atoms in  $n = 2$  levels. The purpose of this paper is twofold. One is to establish the viability of the single-centred expansion coupled-states method for calculating excited state cross sections. Then in later publications we plan to apply this method to other excited state collision systems, particularly those of importance in fusion plasmas.

But a second reason for this paper is to present our results for this collision system. We are aware of no experimental data and there is only very limited previous theoretical work. We report cross sections for the individual  $2s$  and  $2p$  initial states as well as the cross sections averaged over all  $n = 2$  initial state sublevels, assuming that each sublevel is equally populated. Previous calculations have focused on the latter. But in a low density situation a population of  $2s$  metastable states might be experimentally realizable. In high density hydrogen atom environments the distribution of excited atoms between  $2s$  and  $2p$  states might not be statistical and both  $2s$  and  $2p$  cross sections would be needed. For example, in a recent analysis of the role of  $H(n = 2)$  in highly dissociated hydrogen plasmas Geddes and McCullough (1993) argue that atoms formed in the  $2s$  state are rapidly converted to the  $2p$  state by collision and that a large population of the  $2p$  state can be maintained despite its short natural radiative lifetime by radiation trapping. And of course the individual  $2l \rightarrow n'l'$  cross sections are a more sensitive test of theory than are the  $n = 2 \rightarrow n'$  cross sections obtained by summing over degenerate final states and averaging over degenerate initial states.

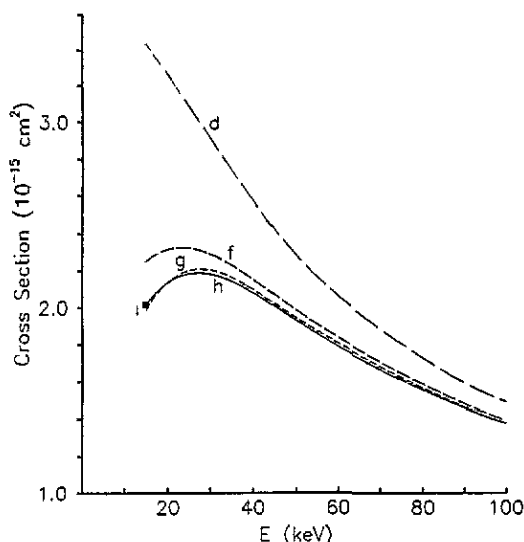


**Figure 1.** Angular momentum convergence of the  $n = 2 \rightarrow n' = 3$  excitation cross section. Each curve is labelled with the maximum  $l$  used in the basis. One point at 15 keV for  $l_{\max} = 6$  (i states) is shown. Excellent convergence is obtained at 15 keV and above if up through  $l = 5$  (h states) are included in the basis.

## 2. Method

The calculations were carried out using the same methods and basis sets used in Ford *et al* (1993), in fact these excited state cross sections were calculated in the same computer runs that produced the H(1s) cross sections. Several convergence tests were performed for the specific cross sections reported in the next section, similar to the convergence tests performed for the H(1s) cross sections. One is the convergence in  $l_{\max}$ , the maximum angular momentum included in the basis. The single-centred expansion method works if the target centred basis is capable of adequately expanding projectile centred orbitals out to the maximum projectile-target separations at which transitions occur. This requires increasingly more angular momenta as the collision energy is lowered and the charge transfer cross section increases. The convergence of the  $n = 2 \rightarrow n' = 3$  excitation cross section in  $l_{\max}$  is shown as a function of energy in figure 1. There is good convergence at 15 keV and above if up through h states ( $l = 5$ ) are included. The convergence in  $l_{\max}$  is somewhat more rapid for this transition than in the  $1s \rightarrow n' = 2$  case presented in Ford *et al* (1993).

We have also looked at the convergence of the time evolution calculation in the number of time grid points. The results reported here used 181 points and runs with 121 and 341 points were used to test convergence. This time grid convergence was somewhat worse for these excited state cross sections than for the ground state cross sections. By comparing results obtained with different number of time grid points, we estimate that the first Born matrix elements are converged to at worst 2% and much better for most transitions. At 15 keV some of the individual coupled states cross sections are converged only to 6% but at higher energies the convergence is much better, more like 1% or 2%.

Convergence in the number of radial functions in the basis for each  $l$  was tested two ways. One was to repeat the calculation at a few collision energies using 17 rather than 13 radial functions. The excitation cross sections changed by less than 1%. The change in the electron removal cross sections was 3 to 4% at 15 keV but less at higher

energies, for example less than 1% at 100 keV. The second basis convergence test was to examine how accurately our basis describes the initial and final states by comparing the first Born excitation cross sections computed with our basis to PWBA cross sections evaluated analytically using the exact wavefunctions. Agreement was at worst to within 1.5%. We also compared the first Born ionization cross sections calculated with our pseudostates, to the exact PWBA cross sections tabulated by Benka and Kropf (1978). Here the agreement is less good. Our 2s ionization cross sections are 7 to 11% lower than the cross sections extracted from the PWBA tables and our 2p ionization cross sections are 2 to 5% lower, for energies from 15 to 300 keV. The  $n = 2$  ionization cross section (statistical average of 2s and 2p ionization) is 4 to 6% lower. This discrepancy is presumably due to a combination of several factors. One is that the PWBA tables are constructed for application to many-electron atoms for which electron screening is included. The numerical tables must be interpolated to extract numbers appropriate to the pure Coulomb case. Benka and Kropf claim that this interpolation is accurate to 2%. An intrinsic difficulty in calculating ionization using pseudostates is in making the separation between excitation and ionization. Pseudostates lying in energy just above or just below the ionization threshold represent an admixture of bound and continuum states. In our calculations we counted transitions to pseudostates above the ionization energy as being purely ionization and transitions to states below this energy as not contributing at all to ionization. The close agreement between the 13 and 17 state results, where there are a different number of bound pseudostates, would appear to confirm that in our calculation this separation between excitation and ionization is being made accurately. Another source of error in our first Born ionization is our truncation in  $l$  of the basis. Our first Born cross sections were calculated using up through  $l = 6$  (i states). For 2s ionization, in our calculation, h states contribute 5% to 7% and i states 3% to 4%. For 2p ionization, h states contribute 5% and i states 2 to 3%. Our first Born ionization cross sections would be increased somewhat if more  $l$  values were included in the basis.

Including all sources of error we estimate that our excitation cross sections are accurate to within 10% at 15 keV and to within 5% at higher energies. The  $n = 2 \rightarrow n'$  summed and averaged cross sections are better converged than the individual  $2l \rightarrow n'l'$  cross sections, and the largest per cent error is in the smaller cross sections. The error in the 2s electron removal cross section could be as large as 15% at 15 keV and 10% at higher energies, but the error in the 2p and  $n = 2$  electron removal cross sections should be no more than 10% at 15 keV and approximately 5% at higher energies.

As for the 1s initial state cross sections, we were unable to obtain converged results at collision energies below 15 keV. The difficulty appears to be due both to the convergence in  $l_{\max}$  and also in the number of time integration mesh points.

### 3. Results and discussion

Our cross sections for  $2s$  and  $2p \rightarrow 3l'$  excitation are presented in tables 1 and 2. The  $2l \rightarrow 3l'$  cross sections are summed over final state  $m'$  values and averaged over the initial state  $m$  values,

$$\sigma(2l \rightarrow 3l') = \left( \frac{1}{2l+1} \right) \sum_m \sum_{m'} \sigma(2lm \rightarrow 3l'm'). \quad (1)$$

We have tabulations of the individual  $\sigma(2lm \rightarrow 3l'm')$  cross sections that can be provided upon request. The  $\sigma(2l \rightarrow n' = 3)$  cross section is given by

$$\sigma(2l \rightarrow n' = 3) = \sum_{l'} \sigma(2l \rightarrow 3l') \quad (2)$$

Table 1. Cross sections for  $2s$  and  $2p \rightarrow 3l'$  excitation (in units of  $10^{-16} \text{ cm}^2$ ) as a function of the collision energy. In each case the cross sections are summed over all the degenerate sublevels of the indicated final state and averaged over the degenerate sublevels of the initial state.

	15 keV	30 keV	45 keV	60 keV	80 keV	100 keV	125 keV
$2s \rightarrow 3s$	3.44	2.80	2.19	1.76	1.38	1.13	0.919
$2s \rightarrow 3p$	4.69	7.18	7.60	7.35	6.79	6.25	5.60
$2s \rightarrow 3d$	11.0	9.54	7.64	5.83	4.52	3.72	2.99
$2s \rightarrow n' = 3$	19.1	19.5	17.4	14.9	12.7	11.1	9.51
$2p \rightarrow 3s$	0.703	0.413	0.328	0.282	0.242	0.215	0.188
$2p \rightarrow 3p$	5.09	3.59	2.63	2.05	1.57	1.27	1.02
$2p \rightarrow 3d$	14.7	18.6	18.0	16.6	14.7	13.2	11.6
$2p \rightarrow n' = 3$	20.5	22.6	21.0	18.9	16.5	14.7	12.8
$n = 2 \rightarrow n' = 3$	20.2	21.8	20.1	17.9	15.6	13.8	12.0

Table 2. Approach of the  $2s$  and  $2p \rightarrow 3l'$  excitation cross sections to the first Born as the collision energy  $E$  is increased. For each  $E$  the cross section  $\sigma$  (in units of  $10^{-16} \text{ cm}^2$ ) and the per cent deviation from first Born,  $\Delta = (\sigma - \sigma_{\text{Born}})/\sigma_{\text{Born}}$ , are given.

	100 keV		150 keV		200 keV		300 keV	
	$\sigma$	$\Delta$ (%)	$\sigma$	$\Delta$ (%)	$\sigma$	$\Delta$ (%)	$\sigma$	$\Delta$ (%)
$2s \rightarrow 3s$	1.13	-1.2	0.773	+0.7	0.584	+1.1	0.391	+1.1
$2s \rightarrow 3p$	6.25	-17	5.08	-10	4.27	-7.3	3.26	-4.5
$2s \rightarrow 3d$	3.72	+2.9	2.52	+4.2	1.88	+3.6	1.25	+2.7
$2s \rightarrow n' = 3$	11.1	-9.3	8.37	-5.3	6.74	-3.8	4.90	-2.3
$2p \rightarrow 3s$	0.215	-11.3	0.168	-7.4	0.139	-5.61	0.105	-3.7
$2p \rightarrow 3p$	1.27	+0.8	0.854	+1.4	0.641	+1.2	0.427	+0.8
$2p \rightarrow 3d$	13.2	-13	10.3	-8.2	8.50	-5.8	6.34	-3.5
$2p \rightarrow n' = 3$	14.7	-12	11.4	-7.5	9.28	-5.3	6.87	-3.3
$n = 2 \rightarrow n' = 3$	13.8	-12	10.6	-6.6	8.64	-5.1	6.38	-3.1

and the  $\sigma(n = 2 \rightarrow n' = 3)$  cross section is averaged over the initial state  $l$  value,

$$\sigma(n = 2 \rightarrow n' = 3) = \frac{1}{4} (\sigma(2s \rightarrow n' = 3) + 3\sigma(2p \rightarrow n' = 3)). \quad (3)$$

Tables 1 and 2 show that the  $3d$  cross sections dominate at low energy and that the dipole-allowed transitions have the largest cross sections at high energies. The  $2s \rightarrow n' = 3$  and  $2p \rightarrow n' = 3$  cross sections are approximately equal at the lower energies but the  $2p \rightarrow n' = 3$  cross section is larger than  $2s \rightarrow n' = 3$  at higher energies. Table 2 shows the approach of the cross sections to first Born as the collision energy increases. Some of the  $2l \rightarrow 3l'$  cross sections approach the first Born from below and some from above, but the cross sections that differ most from first Born approach it from below. The  $2l \rightarrow 3l'$  cross sections, where  $l$  does not change, are already very close to first Born at 100 keV.

We do not know of any published results with which we can compare for the  $2l \rightarrow 3l'$  cross sections. Our  $n = 2 \rightarrow n' = 3$  averaged and summed cross section is compared to some other theoretical calculations in figure 2. Our coupled states calculation is compared to the first Born and to two other calculations: the single-centred atomic orbital (AO) calculations of Reinhold *et al* (1990), at energies of 40 keV and above and to the asymptotic adiabatic method results of Janev and Krstic (1992), which extend up to 20 keV. The Janev and Krstic results are a little lower than ours in the small energy region where the two

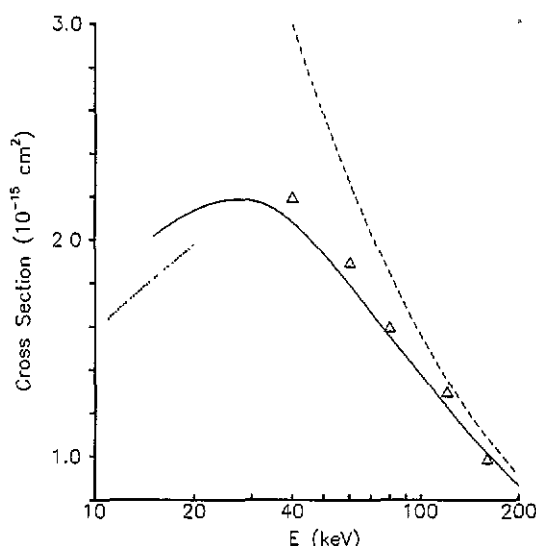


Figure 2. The  $n = 2 \rightarrow n' = 3$  excitation cross section. The full curve is the present calculation and the broken curve is the first Born approximation. The open triangles are the single-centred expansion calculation of Reinhold *et al* (1990). The dotted curve at low energies is the asymptotic adiabatic method result of Janev and Krstic (1992).

calculations overlap. As was the case for excitation from  $H(1s)$  (Ford *et al* 1993) the results of Reinhold *et al* are in close agreement with ours. They used a basis of 74 orbitals that included all hydrogen atom bound states up through  $n = 5$ , so must have had  $l$  values at least up through  $l = 4$  (g states), plus continuum pseudostates. They also performed CTMC and symmetrical eikonal calculations, both of which are in good agreement with their AO results and also with our calculation.

Table 3. Cross sections for  $2s$  and  $2p \rightarrow 4l'$  excitation (in units of  $10^{-16} \text{ cm}^2$ ) as a function of the collision energy. As in table 1 the cross sections are summed over final state degeneracies and averaged over initial state degeneracies.

	15 keV	30 keV	45 keV	60 keV	80 keV	100 keV	125 keV
$2s \rightarrow 4s$	0.723	0.618	0.470	0.373	0.289	0.233	0.188
$2s \rightarrow 4p$	0.836	1.22	1.34	1.31	1.22	1.13	1.02
$2s \rightarrow 4d$	1.22	1.03	0.824	0.668	0.527	0.437	0.356
$2s \rightarrow 4f$	1.87	1.23	0.784	0.550	0.384	0.294	0.225
$2s \rightarrow n' = 4$	4.65	4.09	3.42	2.90	2.42	2.10	1.79
$2p \rightarrow 4s$	0.193	0.0898	0.0669	0.0557	0.0468	0.0412	0.0358
$2p \rightarrow 4p$	1.16	0.778	0.554	0.423	0.320	0.256	0.205
$2p \rightarrow 4d$	2.14	2.70	2.66	2.44	2.16	1.93	1.69
$2p \rightarrow 4f$	1.51	1.27	0.936	0.705	0.517	0.409	0.318
$2p \rightarrow n' = 4$	4.99	4.83	4.22	3.63	3.04	2.64	2.25
$n = 2 \rightarrow n' = 4$	4.91	4.65	4.02	3.45	2.89	2.50	2.13

Tables 3 and 4 and figure 3 give similar results and comparisons for  $2l \rightarrow 4l'$  excitation. Applying  $1/n^3$  scaling to the  $n' = 3$  excitation cross sections gives  $n' = 4$  excitation cross sections approximately a factor of two larger than what we calculate, both in first Born and also in the coupled states calculation. The  $2s \rightarrow 4f$  and  $2p \rightarrow 4f$  cross sections are large at

**Table 4.** Approach of the  $2s$  and  $2p \rightarrow 4l'$  excitation cross sections to the first Born as the collision energy  $E$  is increased. The cross section  $\sigma$  is in units of  $10^{-16} \text{ cm}^2$  and as in table 2,  $\Delta$  is the per cent deviation from first Born.

	100 keV		150 keV		200 keV		300 keV	
	$\sigma$	$\Delta$ (%)	$\sigma$	$\Delta$ (%)	$\sigma$	$\Delta$ (%)	$\sigma$	$\Delta$ (%)
$2s \rightarrow 4s$	0.233	+4.2	0.157	+4.6	0.118	+4.0	0.0780	+3.0
$2s \rightarrow 4p$	1.13	-17	0.928	-10	0.780	-7.4	0.593	-4.6
$2s \rightarrow 4d$	0.437	-3.5	0.303	+0.07	0.229	+0.6	0.153	+0.9
$2s \rightarrow 4f$	0.294	+22	0.185	+15	0.133	+10	0.0853	+6.2
$2s \rightarrow n' = 4$	2.10	-8.2	1.57	-4.6	1.26	-3.4	0.909	-2.1
$2p \rightarrow 4s$	0.0412	-11	0.0320	-6.9	0.0262	-5.4	0.0195	-3.6
$2p \rightarrow 4p$	0.256	+3.4	0.171	+3.1	0.128	+2.3	0.0846	+1.5
$2p \rightarrow 4d$	1.93	-13	1.51	-7.8	1.23	-5.5	0.910	-3.3
$2p \rightarrow 4f$	0.409	+26	0.260	+18	0.188	+13	0.120	+8.1
$2p \rightarrow n' = 4$	2.64	-7.1	1.97	-4.1	1.57	-3.0	1.13	-1.9
$n = 2 \rightarrow n' = 4$	2.50	-7.4	1.87	-4.2	1.50	-3.0	1.08	-1.9

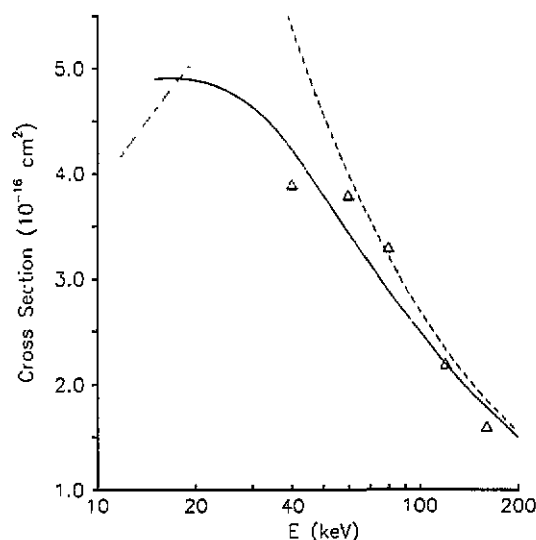


**Figure 3.** The  $n = 2 \rightarrow n' = 4$  excitation cross section. The same notation as in figure 2 is used.

the lower energies and show large positive deviations from first Born at the higher energies (table 4). The agreement with the Reinhold *et al* calculations (figure 3) is somewhat less good than it is for  $n' = 3$  excitation.

Our single-centred expansion calculations do not give separate charge transfer and ionization cross sections, but we found in Ford *et al* (1993) that they do give accurate results for the sum of these cross sections, the electron removal cross section. Our results are given in table 5. At each energy the calculation is done with an  $l_{\text{max}}$  that produces good convergence in the coupled-states calculation and then the first Born ionization cross section calculated with our basis is added for all higher  $l$  values up through  $l = 6$  (i states). Table 5 shows that the electron removal cross section rapidly approaches the first Born ionization cross section, from above, as the collision energy is increased.

**Table 5.** Cross sections for electron removal from  $H(2s)$  and  $H(2p)$  (in units of  $10^{-16} \text{ cm}^2$ ) as a function of the collision energy. For the  $2p$  initial state the cross section is averaged over the three  $m$  components of this state. The averaging over the initial state gives  $\sigma(n=2) = \frac{1}{4}(\sigma(2s) + 3\sigma(2p))$ . The quantity  $\Delta$  is the per cent difference between the electron removal cross section and the first Born ionization cross section calculated in our basis including up through  $l = 6$  states. That is,  $\Delta = (\sigma - \sigma_{\text{Born}})/\sigma_{\text{Born}}$ .

	15 keV	30 keV	45 keV	60 keV	80 keV	100 keV	125 keV
$\sigma(2s)$	25.1	14.7	10.4	8.11	6.31	5.22	4.29
$\Delta$ (%)	8.1	5.5	3.0	1.7	0.9	0.8	0.5
$\sigma(2p)$	31.7	18.9	12.9	9.84	7.50	6.12	4.97
$\Delta$ (%)	16	13	7.9	5.2	3.3	2.8	2.1
$\sigma(n=2)$	30.0	17.9	12.3	9.41	7.20	5.89	4.80
$\Delta$ (%)	14	11	6.8	4.5	2.7	2.4	1.7

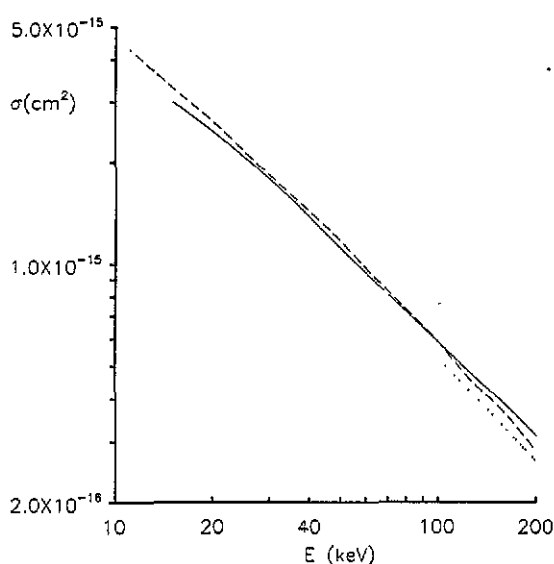


**Figure 4.** The  $H(n=2)$  electron removal cross section. The full curve is the present calculation. The broken curve is the CTMC result of Olson (1980). The dotted curve at high energies is the high-energy limiting form given by Olson (1980):  $\sigma = 24\pi a_0^2/v^2$  where  $v$  is the proton velocity in atomic units.

The only previous calculation of electron removal from  $H(n=2)$  we find in the literature is the CTMC calculation of Olson (1980). His results are compared to ours in figure 4 and the agreement is seen to be excellent. Also shown is the high energy limit given by Olson:  $\sigma = 6\pi a_0^2 n^2/v^2$ , where  $v$  is the proton projectile velocity in atomic units. Olson calculates the separate capture and ionization components of the removal cross section. In his results capture dominates at low energies but falls off rapidly and soon becomes negligible as the energy is increased. His result for capture is 86% of the total at 6.3 keV but its per cent contribution drops to 27% at 15 keV, to 13% at 20 keV and becomes negligible at higher energies. There have been a few other recent calculations of either ionization or capture separately. Janev and Krstic (1992) have calculated ionization cross sections for the individual  $2s$  and  $2p$  states but only for energies up to 20 keV. Their average  $n=2$  ionization is in good agreement with Olson's CTMC in the narrow energy range (6.3 to

20 keV) where they overlap. Fainstein *et al* (1990) used the continuum distorted-wave-eikonal initial-state model (CDW-EIS) to calculate ionization of  $H(n=2)$ . The cross section in figure 1 of their paper must be divided by the initial state degeneracy of 4 to get what we have defined as the  $\sigma(n=2)$  ionization cross section. Their ionization results agree reasonably well with the CTMC results of Olson near the cross section maximum at around 20 keV but their results become larger than Olson's as the energy is increased: a factor of 1.5 larger at 30 keV and a factor of 2 larger at 100 keV. Therefore, at energies of 30 keV and above where charge capture can be neglected and the electron removal and ionization cross sections are essentially the same, their CDW-EIS calculation also disagrees with ours. Electron capture from  $H(2s)$  has been calculated by Reinhold and Miraglia (1987) from 1 to 200 keV by close coupling and by CTMC. At 15 keV their capture cross section is 24% of our  $H(2s)$  electron removal cross section, but there is no calculation of the  $H(2s)$  ionization cross section at this energy. Very recently Esry *et al* (1993) have used the close-coupling method to calculate electron capture from  $H(2s)$  and  $H(2p)$  but the highest energy for which they reported results was 16 keV.

In summary, we have presented results of single-centred expansion coupled-states calculations of excitation and electron removal for  $p + H(2s)$  and  $p + H(2p)$  collisions in the 15 keV to 300 keV energy region. There are no previously published calculations for the  $2s$  and  $2p$  initial states. Our cross sections for the average  $n=2$  initial state are in good agreement with other available calculations. Our calculations were driven to convergence in the maximum angular momentum included in the basis and when this is done we find that the single-centred expansion method gives accurate cross sections even in situations where charge transfer is large. Our results establish this method as being useful for calculating excited state cross sections in the intermediate energy regime. We also hope that our presentation of cross sections between specific states will be useful in plasma fusion modelling and that our results will be useful for comparison to other calculations done in the future and even perhaps to experiment.

## Acknowledgments

This work was supported by the US National Science Foundation under grant PHY-9009717 and by the Department of Energy under grant DE-FG05-92ER54174. We thank Carlos Reinhold for providing a numerical tabulation of the AO results of Reinhold *et al* 1990.

## References

- Benka O and Kropf A 1978 *At. Data Nucl. Data Tables* **22** 219–33
- Esry B D, Chen Z, Lin C D and Piacentini R D 1993 *J. Phys. B: At. Mol. Opt. Phys* **26** 1579–86
- Fainstein P D, Ponce V H and Rivarola R D 1990 *J. Phys. B: At. Mol. Opt. Phys* **23** 1481–9
- Ford A L, Reading J F and Hall K A 1993 *J. Phys. B: At. Mol. Opt. Phys* **26** 4537–51
- Geddes J and McCullough R W 1993 *J. Phys. B: At. Mol. Opt. Phys* **26** L165–8
- Janev R K and Krstic P S 1992 *Phys. Rev. A* **46** 5554–77
- Olson R E 1980 *J. Phys. B: At. Mol. Phys* **13** 483–92
- Reinhold C O and Miraglia J E 1987 *J. Phys. B: At. Mol. Phys* **20** 541–9
- Reinhold C O, Olson R E and Fritsch W 1990 *Phys. Rev. A* **41** 4837–42